Multiscale Modeling of Piezoelectric Materials

Lieutenant Colonel Steven L. Creighton, Ph.D.
Department of Civil & Mechanical Engineering
United States Military Academy
West Point, New York

Dr. Peter Chung
Team Leader, Interdisciplinary Sciences Team
Computational & Information Sciences Directorate
Army Research Laboratory (ARL)
Aberdeen, MD

Dr. John D. Clayton
Research Scientist, Impact Physics Branch
Weapons and Materials Research Directorate
Army Research Laboratory (ARL)
Aberdeen, MD

Abstract

Piezoelectric materials possess tremendous potential in twenty-first century engineering applications. A high-fidelity model is sought that can more accurately predict piezoelectric behavior by embedding parameters typically associated with the fine scale (i.e. atomic scale) into contemporary piezoelectric macro scale formulation. The research presented is theoretical and demonstrates how this can be realized. The material examined is lead-zirconate-titanate (PZT). The model presented utilizes an energy potential based on atomistic attractive forces to develop an elastic modulus that is incorporated into classical macro scale piezoelectric governing equations – in-lieu-of the standard elasticity tensor. Also presented will be ideas for future work where-by the atomistic modulus is utilized in a variational multiscale environment.

1 Introduction

Piezoelectric materials possess the unique property that when subjected to a deformation they produce electricity. Conversely, when these materials are subjected to an electric field, they undergo deformation. This unique property has been exploited by researchers and engineers to achieve desired effects – such as in the design of the ignition system in the rocket propelled grenade launcher (RPG) – shown in Figure 1.2 – and continues to intrigue researchers with its promise in the design of new systems and devices. New piezoelectric applications are limited only by the imagination. Figure 1.1 below shows rotor blade research conducted at the University of Maryland in an attempt to design smart controllable blades that have desirable twist characteristics.

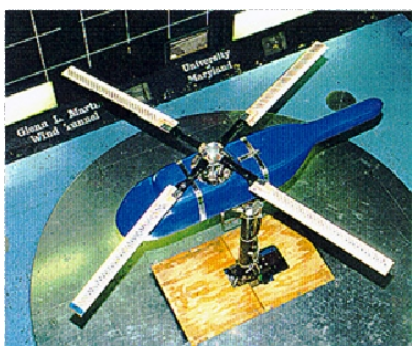

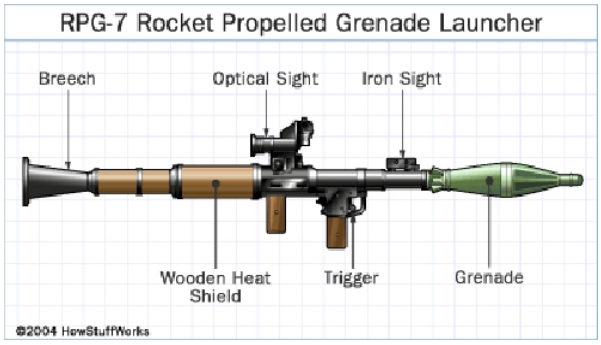

Figure 1.1 Smart controllable rotorcraft twist research. http://www.enae.umd.edu/AGRC/pict/	**Figure 1.2** Rocket Propelled Grenade launcher. http://science.howstuffworks.com/rpg3.htm

At the United States Military Academy (USMA), students and researchers (Labo, 2005) have researched the incorporation of piezoelectric materials in combat boots (See Figure 1.3 and Figure 1.4). This research was motivated by an attempt to capture the excess energy that is generated during the natural gait of a soldier's step. Other uses of piezoelectric materials include sophisticated power generation systems for micro sensors

and micro-electro-mechanical systems (MEMS) devices,; and household uses such as ignition switches for propane barbeque grills.

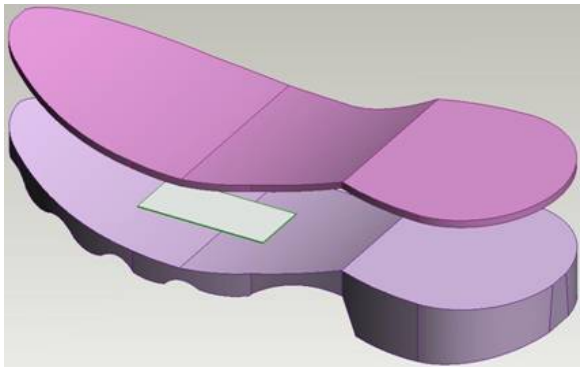

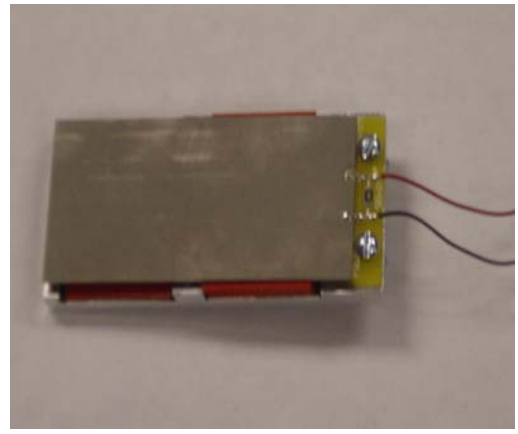

Figure 1.3 Piezoelectric board inserted into a combat boot.	**Figure 1.4** Piezoelectric board.

2 PZT Monoclinic Structure

The introduction to piezoelectric materials mentioned above motivates an explanation of how piezoelectric materials work. To do this,, the molecular make up of these materials must be examined. To limit the scope of this explanation – and stay within the context of the research at hand – the piezoelectric material $PbZr_{0.52}Ti_{0.48}O_3$ will be discussed. The material $PbZr_{0.52}Ti_{0.48}O_3$ (see Figure 2.1) is a subset of piezoelectric materials called PZTs that contain lead (Pb), zirconim (Zi), and titanium (Ti). This material is also a subset of materials called Perovskites that are composed of atoms of the form ABO_3. In $PbZr_{0.52}Ti_{0.48}O_3$, Pb is the A atom and either Zr or Ti (randomly distributed) is the B atom.

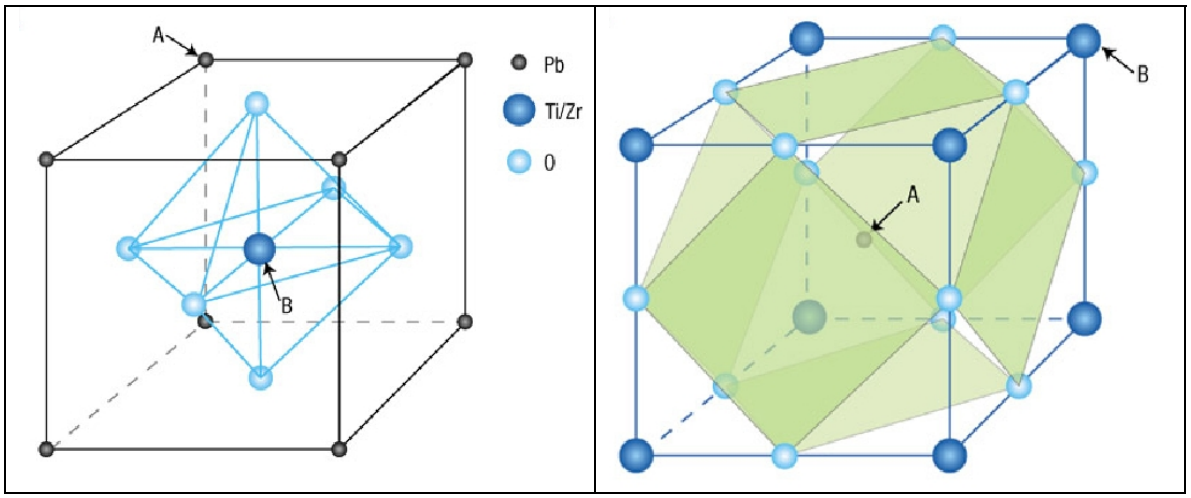

Figure 2.1 The $PbZr_{0.52}Ti_{0.48}O_3$ (PZT) molecule (Rabe, 2002).

The author of Figure 1.1 (Rabe, 2002). aptly describe this molecule's behavior as follows:

> **The ideal perovskite structure (ABO_3) centred on a, the B site (Ti/Zr) and b, the A site (Pb).** In the piezoelectric material PZT the Zr and Ti atoms are randomly distributed on the B sites. Using first-principles calculations Grinberg and colleagues[2] show that each Pb atom displaces preferentially towards square green faces with the largest Ti fraction. These local distortions can be correlated with global structure and behaviour. For example, in PZT the displacement of the metal ions (Pb, Ti and Zr) away from the centre of their oxygen cages generates local polarization and ultimately ferroelectricity. **c**, The net polarization and overall structure of PZT changes with the ratio of Ti:Zr atoms, as shown in the $x-T$ phase diagram. The six structural phases of PZT at ambient pressure are mostly ferroelectric, with the exception of antiferroelectric behaviour (A) near $PbZrO_3$ and a paraelectric cubic phase (C) at high temperatures. Grinberg *et al*. show that the complex phase behaviour of different Zr/Ti compositions can be explained by averaging the changing distribution of Pb displacements, which depend on their local environment. T = Ti-rich tetragonal phase; R = rhombohedral phase; M = monoclinic ferroelectric phase.

3 Notation

The following portion of this paper concerns itself with incorporating the piezoelectric behavior of the PZT molecule shown above into a mathematical formulation which can in turn be implemented by computational methods. It is appropriate at this point to make clear distinction of the notation used throughout the rest of this paper. To discern between scalar and tensoral variables, we will use the standard indicial notation u_i for first order tensors (i.e. vector variables), u_{ij} for second order tensors, u_{ikj} for third order tensors, and so on. In a 3D calculation, all tensor and vector indices span the range (1,2,and 3). Variables with no indices will be understood to be scalar quantities.

Moreover, variables in bold font (e.g. $\mathbf{u}$) will be understood to be tensor variables (order implied by usage) and unbold font will imply scalar quantities. When discussing atomistic relationships, atom labels will be denoted by the lone indices i, j, or k in parentheses, usually as superscripts. For example, $\mathbf{r}^{(ij)}$ (or $\mathbf{r}(i, j)$) is the position vector from atom *i* to atom *j* (see Figure 5.1).

In this paper, the term *fine-scale* refers to events occurring at atomistic scales on the order of ten Angstroms, while the term *macro-scale* refers to events occurring at scales larger than 100 microns (i.e. visible to the naked eye). The term *coarse-scale* is also seen in the paper and is to have a meaning synonymous with macro-scale.

4 Atomistic Behavior and the Constitutive Equation

In formulating mathematical equations to model the physical world, material properties are incorporated via constitutive equations. The classical constitutive equation used in solid mechanics on the macro-scale is Hooke's Law and the tensor variable possessing the material behavior is the Elasticity Tensor denoted C_{IJKL}. Hooke's Law is stated as:

$$S_{IJ} = C_{IJKL} E_{KL}$$

where S_{IJ} is the stress tensor and E_{KL} the strain tensor. In a loose sense, S_{IJ} embodies the forces acting on a body while E_{KL} embodies the displacements that occur as a result of these forces. It is a reasonable assumption, therefore, that if material behavior normally associated with the PZT fine-scale is to be mathematically embedded into equations describing the macro-scale, the elasticity tensor seen in Hooke's law is where the embedding should occur. Needed for the research at hand is the formulation of an elasticity tensor which encapsulates PZT atomistic behavior.

5 Atomistic Elasticity Tensor

5.1 Atomistic Kinematics

Figure 5.1.1 depicts three atoms i, j, and k in the reference and current configurations. These atoms are located by Cartesian position vectors $\mathbf{X}^{(IJ)}, \mathbf{X}^{(IK)}, \mathbf{X}^{(JK)}$ and $\mathbf{x}^{(ij)}, \mathbf{x}^{(ik)}, \mathbf{x}^{(jk)}$ in the reference and current configurations respectively. The atoms may locally be described by their proximity to each other by the position vectors $\mathbf{R}^{(IJ)}, \mathbf{R}^{(IK)}, \mathbf{R}^{(JK)}$ and $\mathbf{r}^{(ij)}, \mathbf{r}^{(ik)}, \mathbf{r}^{(jk)}$ also shown in respective configurations.

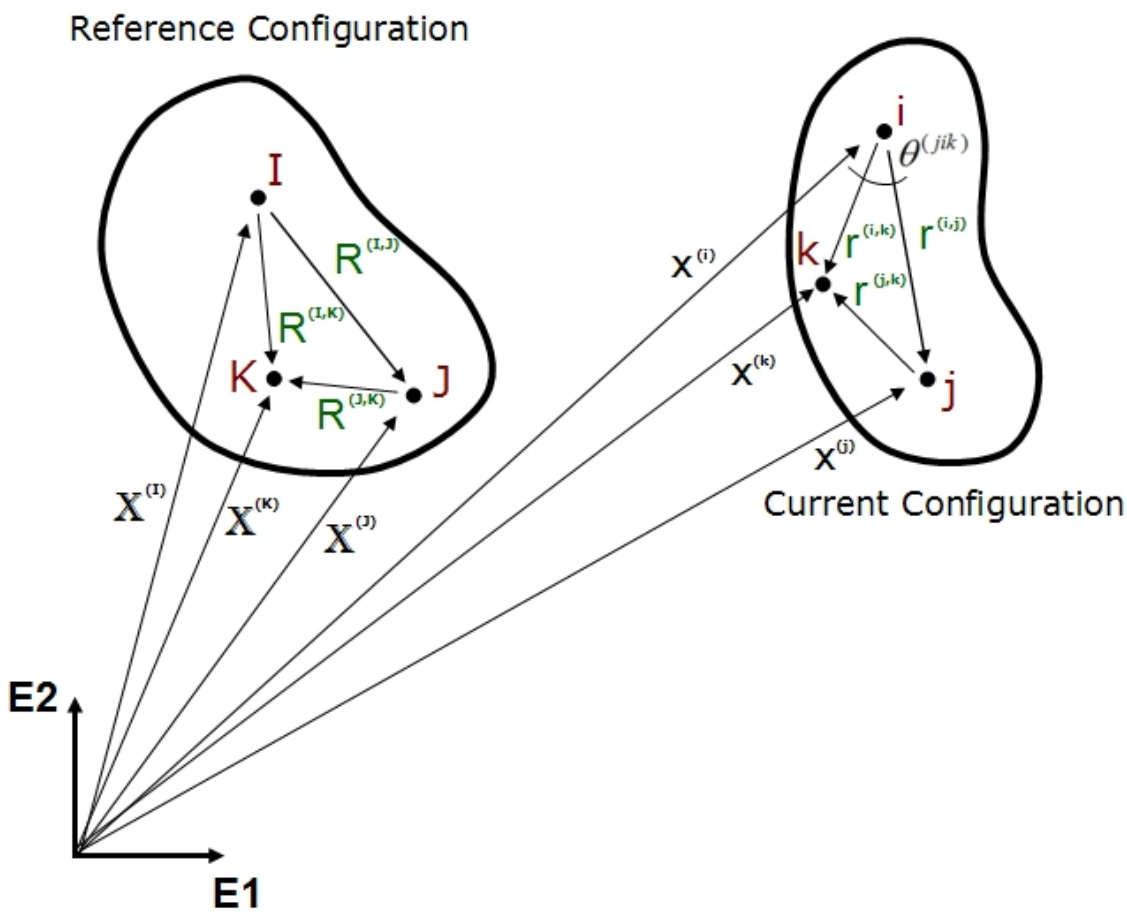

Figure 5.1 Three atoms depicted in the reference and current configurations.

The angle created by two vectors subtending atom *i* is defined by the symbol $\theta^{(jik)} = \theta^{(kij)}$ where the atom subtended is the middle index. The cosine of this angle is therefore

$$\cos\theta^{(jik)} = \frac{\mathbf{r}^{(ij)}}{\left|\mathbf{r}^{(ij)}\right|} \cdot \frac{\mathbf{r}^{(ik)}}{\left|\mathbf{r}^{(ik)}\right|} = \frac{\mathbf{r}^{(ij)}}{r^{(ij)}} \cdot \frac{\mathbf{r}^{(ik)}}{r^{(ik)}},$$

and $r^{(ij)} = \sqrt{\mathbf{r}^{(ij)} \cdot \mathbf{r}^{(ij)}}$.

We note that all kinematic variables defined for any three atoms can be simplified to two vectors. For example, $\theta^{(jik)} = \theta^{(jik)}(\mathbf{r}^{(ij)}, \mathbf{r}^{(ik)})$ and $\mathbf{r}^{(jk)} = \mathbf{r}^{(ik)} - \mathbf{r}^{(ij)}$. Therefore, in what follows, the two truly independent variables are $\mathbf{r}^{(ij)}$ and $\mathbf{r}^{(ik)}$.

5.2 Definition of Potential

The form of the potential is given as

$$\phi = \sum_{\substack{i,j \\ i<j}} v_2(i,j) + \sum_{\substack{i,j,k \\ i<j<k}} v_3(i,j,k) \tag{1}$$

(1)

where the first summation denotes pair interactions and the second summation the interactions of atom triples. Note that there is no factor of ½ contained in the equation because the summation conditions disallow double-counting. The pair and triple terms are defined as

$$\begin{aligned} v_2(i,j) &= \varepsilon f_2(\mathbf{r}^{(ij)}/\sigma) \\ v_3(i,j,k) &= \varepsilon f_3(\mathbf{r}^{(ij)}/\sigma, \mathbf{r}^{(ik)}/\sigma, \mathbf{r}^{(jk)}/\sigma) \end{aligned} \tag{2}$$

where the constant ε is chosen so as to give the minimum of f_2 at -1, and σ is chosen to make $f_2(2^{1/6})$ vanish. These constants are given for Si in (Stillinger and Weber, 1985).

The pair term is a function of the scalar distance between two atoms *i* and *j* defined as

$$f_2(r) = \begin{cases} A(Br^{-p} - r^{-q})\exp[(r-a)^{-1}], & r < a \\ 0, & r \geq a \end{cases} \tag{3}$$

where *A, B, p, q*, and *a* are constants. Noticeable in this equation is that the range of the pair interactions is limited to a circular region of radius *a* around each atom. The triple interaction is defined as

$$f_3(\mathbf{r}^{(ij)}, \mathbf{r}^{(ik)}, \mathbf{r}^{(jk)}) = h(r^{(ij)}, r^{(ik)}, \theta^{(jik)}) + h(r^{(ji)}, r^{(jk)}, \theta^{(ijk)}) + h(r^{(ki)}, r^{(kj)}, \theta^{(ikj)})$$

(4)

where

$$h(r^{(ij)}, r^{(ik)}, \theta^{(jik)}) = \lambda \exp\left[\gamma\left(r^{(ij)} - a\right)^{-1} + \gamma\left(r^{(ik)} - a\right)^{-1}\right]\left[\cos\theta^{(jik)} + \tfrac{1}{3}\right]^2$$

(5)

Based on the discussion above regarding the fact that there are only two true independent variables, we can redefine *h* in the form of some functions $\overline{h}^{(i)}$ and $h^{(i)}$ so that equation (4) can be rewritten as

$$\begin{aligned} f_3 &= \overline{h}^{(i)}(\left|\mathbf{r}^{(ij)}\right|, \left|\mathbf{r}^{(ik)}\right|) + \overline{h}^{(j)}(\left|\mathbf{r}^{(ji)}\right|, \left|\mathbf{r}^{(jk)}\right|) + \overline{h}^{(k)}(\left|\mathbf{r}^{(ki)}\right|, \left|\mathbf{r}^{(kj)}\right|) \\ &= h^{(i)}(\mathbf{r}^{(ij)}, \mathbf{r}^{(ik)}) + h^{(j)}(\mathbf{r}^{(ji)}, \mathbf{r}^{(jk)}) + h^{(k)}(\mathbf{r}^{(ki)}, \mathbf{r}^{(kj)}) \\ &= h^{(i)}(\mathbf{r}^{(ij)}, \mathbf{r}^{(ik)}) + h^{(j)}(-\mathbf{r}^{(ij)}, \mathbf{r}^{(ik)} - \mathbf{r}^{(ij)}) + h^{(k)}(-\mathbf{r}^{(ik)}, \mathbf{r}^{(ij)} - \mathbf{r}^{(ik)}) \end{aligned} \tag{6}$$

where

$$h^{(i)}(\mathbf{r}^{(ij)}, \mathbf{r}^{(ik)}) = \lambda \exp\left[\gamma\left(\sqrt{\mathbf{r}^{(ij)} \cdot \mathbf{r}^{(ij)}} - a\right)^{-1} + \gamma\left(\sqrt{\mathbf{r}^{(ik)} \cdot \mathbf{r}^{(ik)}} - a\right)^{-1}\right]\left[\frac{\mathbf{r}^{(ij)}}{\left|\mathbf{r}^{(ij)}\right|} \cdot \frac{\mathbf{r}^{(ik)}}{\left|\mathbf{r}^{(ik)}\right|} + \tfrac{1}{3}\right]. \tag{7}$$

5.3 Finite Strain and Classical Continuum Mechanics

The atoms labeled *i*, *j*, and *k* are assumed in the deformed configuration. The equations thus far are only considering the instantaneous configuration to evaluate the energies from equation (1). From a Lagrangian continuum solid mechanics perspective, it is

important to know *how* those atoms got there. We therefore define atoms labeled *I*, *J*, and *K* as the reference configuration relative to the original Cartesian basis.

We consider only affine deformations, meaning that the deformation process at the atomic scale is assumed to work in the same way as the continuum scale. Under this one-to-one mapping assumption, position vectors in the reference configuration **R** get transformed to the current configuration **r** through the deformation tensor **F,**

$$(\mathbf{r})_i = (\mathbf{FR})_i = r_i = \sum_I F_{iI} R_I = F_{iI} R_I \tag{8}$$

where repeated indices are assumed summation.

We use the conventional strain measures for the *Green* strain and *Right Cauchy-Green* strain, respectively as follows

$$\begin{aligned} E_{IJ} &= \tfrac{1}{2}(F_{iI}F_{iJ} - \delta_{IJ}) \\ C_{IJ} &= F_{iI}F_{iJ} \end{aligned} \tag{9}$$

We can then obtain a host of elasticity tensors by taking second derivatives of a strain energy function. From equation (1), the strain energy function is defined by

$$\Phi = \frac{1}{N}\left(\phi(r) - \phi(R)\right) \tag{10}$$

where *N* is the number of atoms. Then different types of elasticity tensors may be determined. For example, we may choose among the following fourth order tensors,

$$\frac{\partial^2\Phi}{\partial C_{IJ}\partial C_{KL}}, \frac{\partial^2\Phi}{\partial E_{IJ}\partial E_{KL}}, \frac{\partial^2\Phi}{\partial F_{iJ}\partial F_{kL}}, \frac{\partial^2\Phi}{\partial \varepsilon_{ij}\partial \varepsilon_{kl}} \tag{11}$$

where the last tensor is based on the infinitesimal strain and would give the standard infinitesimal elastic constants after taking appropriate directional derivatives.

The process for obtaining any of the elastic property tensors is identical. We make repeated use of the chain rule to analytically determine the derivatives. Let us consider the following elastic tensor as the illustrative example,

$$\mathbb{C}_{IJKL} = \frac{\partial^2\Phi}{\partial C_{IJ}\partial C_{KL}} \tag{12}$$

By making use of earlier definitions, we proceed as follows

$$\begin{aligned} \mathbb{C}_{IJKL} &= \frac{\partial^2\Phi}{\partial C_{IJ}\partial C_{KL}} \\ &= \frac{\partial^2\Phi}{\partial F_{mN}\partial F_{pQ}}\frac{\partial F_{mN}}{\partial C_{IJ}}\frac{\partial F_{pQ}}{\partial C_{KL}} \\ &= \left(\begin{aligned} &\frac{\partial^2\Phi}{\partial r_i^{(ij)}\partial r_j^{(ik)}}\frac{\partial r_i^{(ij)}}{\partial F_{mN}}\frac{\partial r_j^{(ik)}}{\partial F_{pQ}} + \frac{\partial^2\Phi}{\partial r_i^{(ij)}\partial r_j^{(ij)}}\frac{\partial r_i^{(ij)}}{\partial F_{mN}}\frac{\partial r_j^{(ij)}}{\partial F_{pQ}} \\ &\quad + \frac{\partial^2\Phi}{\partial r_i^{(ik)}\partial r_j^{(ik)}}\frac{\partial r_i^{(ik)}}{\partial F_{mN}}\frac{\partial r_j^{(ik)}}{\partial F_{pQ}} + \frac{\partial^2\Phi}{\partial r_i^{(ik)}\partial r_j^{(ij)}}\frac{\partial r_i^{(ik)}}{\partial F_{mN}}\frac{\partial r_j^{(ij)}}{\partial F_{pQ}} \end{aligned}\right)\frac{\partial F_{mN}}{\partial C_{IJ}}\frac{\partial F_{pQ}}{\partial C_{KL}} \end{aligned} \tag{13}$$

It is important to recall that the summation convention does not apply to indices in parentheses. To complete the process of equation (13), we use the definition in equation (9) to obtain

$$\frac{\partial F_{pQ}}{\partial C_{KL}} = \left(\frac{\partial C_{KL}}{\partial F_{pQ}}\right)^{-1} = \left(\frac{\partial (F_{iK}F_{iL})}{\partial F_{pQ}}\right)^{-1} = \left(F_{pL}\delta_{QK} + F_{pK}\delta_{QL}\right)^{-1},$$

and equation (8) to obtain

$$\frac{\partial r_i^{(ij)}}{\partial F_{mN}} = \frac{\partial\left(F_{iI}R_I^{(ij)}\right)}{\partial F_{mN}} = \delta_{mi}\delta_{NI}R_I^{(ij)} = \delta_{mi}R_N^{(ij)}.$$

The only task that now remains is to evaluate the derivatives of the strain energy potential Φ with respect to the atomic vectors. This is also a straightforward procedure. We start with the first derivative

$$\begin{aligned}\frac{\partial \phi}{\partial r_p^{(ij)}} &= \frac{\partial}{\partial r_p^{(ij)}}\left(\sum_{\substack{i,j\\ i<j}} v_2(i,j) + \sum_{\substack{i,j,k\\ i<j<k}} v_3(i,j,k)\right)\\ &= \sum_{\substack{i,j\\ i<j}} \frac{\partial v_2}{\partial r_p^{(ij)}} + \sum_{\substack{i,j,k\\ i<j<k}} \frac{\partial v_3}{\partial r_p^{(ij)}}\\ &= \sum_{\substack{i,j\\ i<j}} \varepsilon \frac{\partial f_2}{\partial r^{(ij)}}\frac{\partial r^{(ij)}}{\partial r_p^{(ij)}} + \sum_{\substack{i,j,k\\ i<j<k}} \varepsilon\left(\frac{\partial h^{(i)}}{\partial r_p^{(ij)}} + \frac{\partial h^{(j)}}{\partial r_p^{(ij)}} + \frac{\partial h^{(k)}}{\partial r_p^{(ij)}}\right)\end{aligned}$$

where the derivative in the first term is given by

$$\frac{\partial r^{(ij)}}{\partial r_p^{(ij)}} = \frac{\partial\sqrt{r_q^{(ij)}r_q^{(ij)}}}{\partial r_p^{(ij)}} = \frac{1}{2}\left(\sqrt{r_q^{(ij)}r_q^{(ij)}}\right)^{-1}\cdot 2r_t^{(ij)}\delta_{tp} = \frac{r_p^{(ij)}}{r^{(ij)}}.$$

Note that $\partial r^{(ij)}/\partial r_p^{(ik)} = \partial r^{(ik)}/\partial r_p^{(ij)} = 0$. Also, the derivative of the non-zero part of f_2 is

$$\frac{\partial f_2}{\partial r} = A\exp[(r-a)^{-1}]\left[-Br^{-p}\left(\frac{p}{r} + \frac{1}{(a-r)^2}\right) + r^{-q}\left(\frac{q}{r} + \frac{1}{(a-r)^2}\right)\right]$$

A similar derivative needs to be evaluated for $h^{(i)}$.

Likewise, the key second derivatives that need to be derived are

$$\frac{\partial^2\phi}{\partial r_p^{(ij)}\partial r_q^{(ij)}}, \frac{\partial^2\phi}{\partial r_p^{(ij)}\partial r_q^{(ik)}}, \frac{\partial^2\phi}{\partial r_p^{(ik)}\partial r_q^{(ij)}}, \frac{\partial^2\phi}{\partial r_p^{(ik)}\partial r_q^{(ik)}}$$

which will contain expressions such as

$$\frac{\partial r^{(ij)}}{\partial r_p^{(ij)}\partial r_q^{(ij)}} = \frac{\partial\left(r_p^{(ij)}/r^{(ij)}\right)}{\partial r_q^{(ij)}} = \frac{1}{r^{(ij)}}\delta_{pq} + r_p^{(ij)}\frac{\partial\left(1/r^{(ij)}\right)}{\partial r_q^{(ij)}} = \frac{1}{r^{(ij)}}\left(\delta_{pq} + \frac{r_p^{(ij)}}{r^{(ij)}}\frac{r_q^{(ij)}}{r^{(ij)}}\right).$$

By observation of the equations thus far, the elastic stiffness tensor is fully determined. The remaining task is extensive symbolic manipulations to obtain a closed form expression (if so desired) of the tensor, with repeated use of partial derivatives and chain rule multiplications. Due to the algebraic complexity of the potential function, the final expression is generally lengthy, but still obtainable.

6 Variational Multiscale Formulation

While the Elasticity Tensor formulated in Section 5 will confine the displacement of PZT atoms to proper paths and distances within the atomic lattice, needed is a coupling between these atomic displacements and the electric field $\widetilde{\mathbf{E}}$. Moreover, the governing equations for $\widetilde{\mathbf{E}}$ (i.e. Maxwell's Equations) must be present in the overarching mathematical model since they share a role equal to those of solid mechanics regarding piezoelectric phenomenon. To allow for this, the equations used in this model will be formulated in a variational multiscale framework.

6.1 Multiscale Deformation

In the variational multiscale context, the displacement $\mathbf{u}$ of any point in the body (assumed synonymous with an atom's displacement) is decomposed into two parts $\mathbf{u}^{\alpha}$ and $\mathbf{u}^{\beta}$ whereby $\mathbf{u}^{\alpha}$ is a local displacement on the fine-scale, and $\mathbf{u}^{\beta}$ is a global displacement on the macro-scale. Figure 6.1 shows a pictorial example of this notion

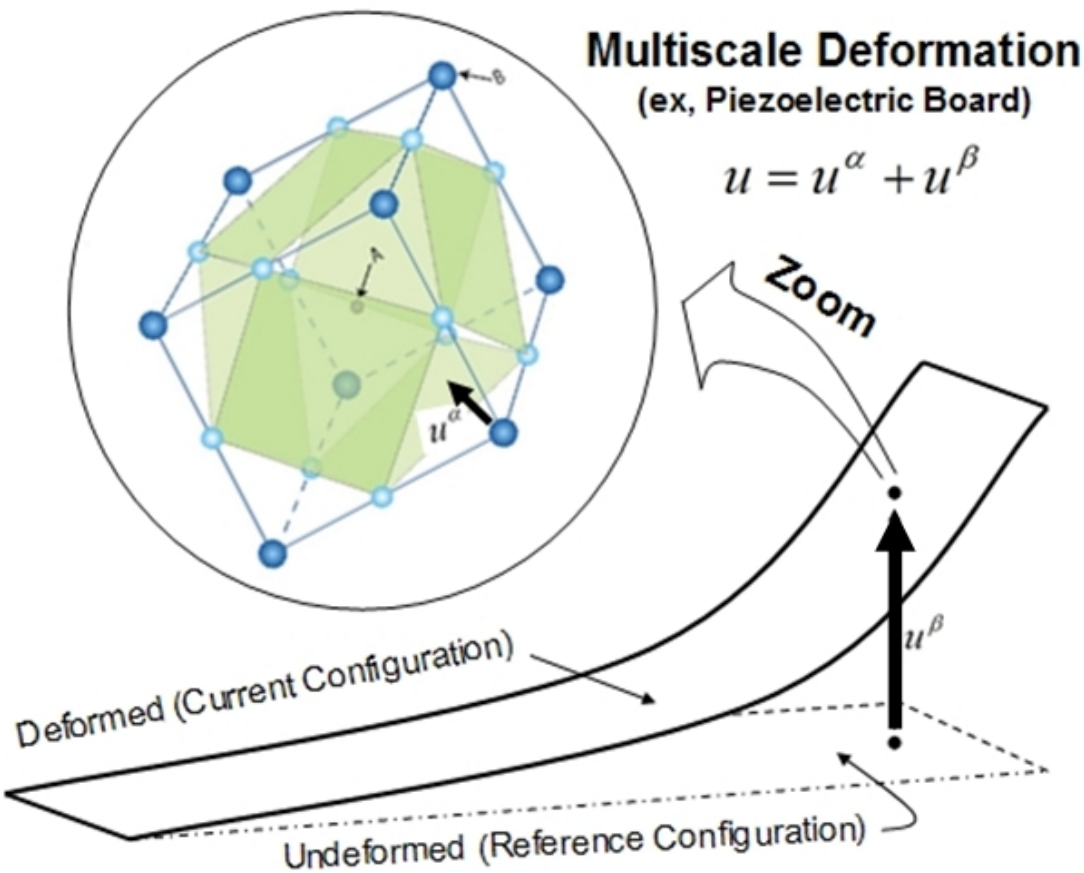

Figure 6.1 Example of multiscale deformation as seen by a piezoelectric board experiencing bending.

Figure 6.2 below demonstrates some additional key points regarding variational multiscale deformation. In Figure 6.2, a hypothetically thin rod is used to demonstrate that: 1) Displacement $\mathbf{u}^{\alpha}$ will have a magnitude on the order of Angstroms, while $\mathbf{u}^{\beta}$ will have a magnitude on the order of meters; 2) Strain is scale independent – a point that will be very important in subsequent sections; and 3) Displacement $\mathbf{u}^{\beta}$ occurs due to the summation of a very large number of fine-scale displacements $\mathbf{u}^{\alpha}$ occurring over the entire body.

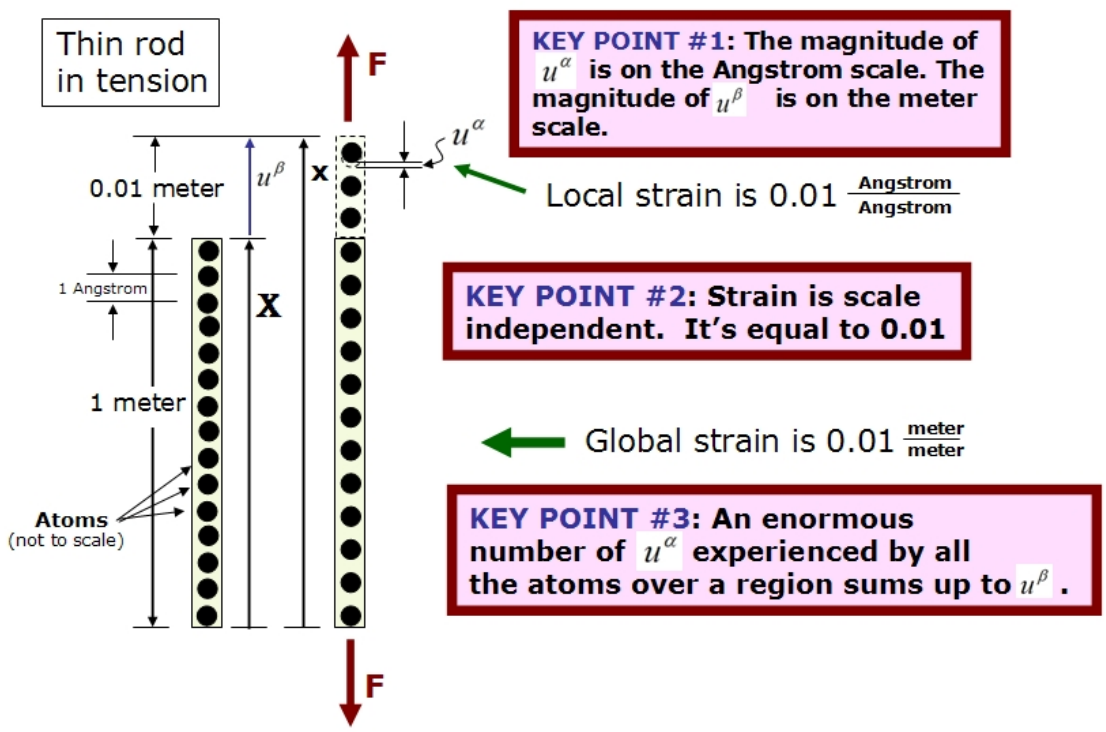

Figure 6.2 Some key points made by observing the deformations in a hypothetical thin wire.

6.2 Multiscale Kinematics

To accommodate fine-scale and coarse-scale equations, an additional intermediate configuration $\bar{\beta}$ is introduced to the two configuration arrangement seen in classical continuum mechanics (See Figure 5.1) . The three configurations are shown in Figure 6.2. In this figure, the position of a point in the intermediate configuration is denoted by $\bar{\mathbf{X}}$.

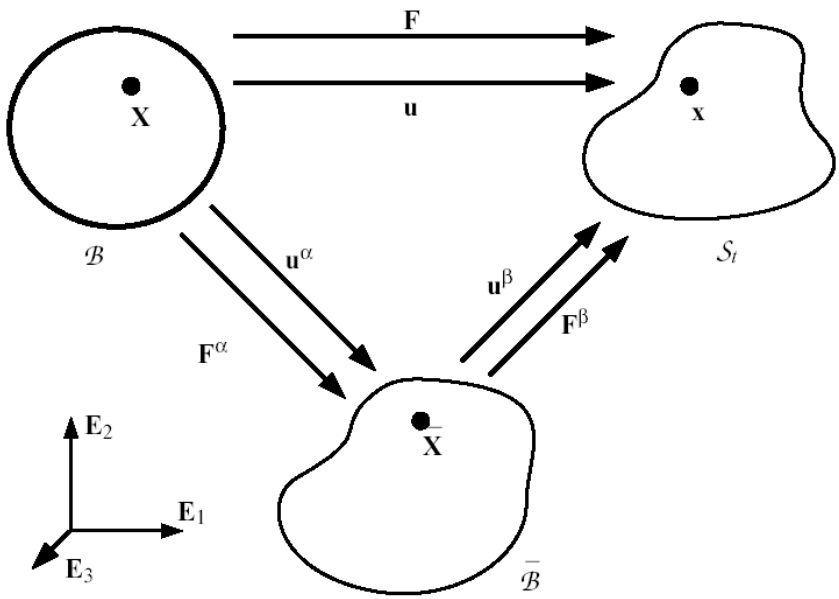

Figure 6.3 Multiscale kinematics. Three configurations are used in this framework – *reference*, *intermediate*, and *current*. (Creighton, 2004).

With these configurations, a logical definition of variables leads to simplistic equations. If displacements are defined as

$$\mathbf{u}^\alpha := \bar{\mathbf{X}} - \mathbf{X}$$

$$\mathbf{u}^\beta := \mathbf{x} - \bar{\mathbf{X}}$$

$$\mathbf{u} := \mathbf{x} - \mathbf{X}$$

then consequently $\mathbf{u} = \mathbf{u}^\alpha + \mathbf{u}^\beta$ as is desired. Defining the deformation gradients as

$$\mathbf{F} := \frac{\mathbf{dx}}{\mathbf{dX}}$$

$$\mathbf{F}^\beta := \frac{\mathbf{dx}}{\mathbf{d}\bar{\mathbf{X}}}$$

$$\mathbf{F}^\alpha := \frac{\mathbf{d}\bar{\mathbf{X}}}{\mathbf{dX}}$$

yields the equations

$$\mathbf{F} = \mathbf{F}^\beta \mathbf{F}^\alpha$$

$$\mathbf{F}^{\alpha} = \mathbf{I} + \frac{\partial \mathbf{u}^{\alpha}}{\partial \mathbf{X}}$$

$$\mathbf{F}^{\beta} = \mathbf{I} - \nabla \mathbf{u}^{\beta}$$

where the nabla symbol represents derivatives taken with respect the current position vector $\mathbf{x}$ such that $\nabla(\bullet) := \frac{\partial(\bullet)}{\partial \mathbf{x}}$. From these equations we define the multiscale Green tensor as

$$\mathbf{E}^{\beta} := \frac{\mathbf{1}}{\mathbf{2}}\left(\mathbf{F}^{\beta^{\mathrm{T}}}\mathbf{F}^{\beta} + \mathbf{1}\right)$$

and the multiscale Right Cauchy-Green tensor as

$$\mathbf{C}^{\beta} := \mathbf{F}^{\beta^{\mathrm{T}}}\mathbf{F}^{\beta}$$

For a rigorous derivation of the variables, in this section see (Creighton, 2004).

6.3 Multiscale Governing Equations of Solid Mechanics

With the kinematic variables defined, we recall macro-scale equations. Equations below are 1) The conservation of linear momentum; 2) A push forward of the *Second Piola-Kirchhoff Stress* tensor **S** to the current configuration; and 3) Hooke's Law. Note the appropriateness of the β superscript in these macro-scale equations (recall that $\mathbf{u}^{\beta}$ is macro-scale displacement).

$$\nabla \cdot \boldsymbol{\sigma} + \mathbf{b} = \boldsymbol{\rho}\ddot{\mathbf{u}}^{\beta} \qquad (6.3.1)$$

$$\boldsymbol{\sigma} = \frac{\mathbf{1}}{\mathbf{J}}\mathbf{F}^{\beta}\mathbf{S}\mathbf{F}^{\beta^{\mathrm{T}}}$$

$$\mathbf{S} = \mathbf{C} : \mathbf{E}^{\beta}$$

Recalling Equation 12 from Section 5, the multiscale version of this equation becomes

$$\mathbf{C} = \frac{\partial^{2}\boldsymbol{\Phi}}{\partial \mathbf{C}^{\beta}\partial \mathbf{C}^{\beta}}$$

It should be noted that using $\mathbf{C}^{\beta}$ in the derivation of the atomistic elasticity tensor $\mathbf{C}$ is appropriate since strains are scale independent (see Key Point #2 in Figure 6.2 to put this

in context). Conversely, incorporating the macro-scale displacement variable $\mathbf{u}^{\beta}$ into the formulation of $\mathbf{C}$ would be inappropriate due to its scale.

6.4 Governing Equations of Electromagnetism

The governing equations for electromagnetism are Maxwell's Equations. From these equations, a relationship for the electric field vector $\widetilde{\mathbf{E}}$ can be written

$$\frac{1}{\mu}\nabla \times \nabla \times \widetilde{\mathbf{E}} + \varepsilon \ddot{\widetilde{\mathbf{E}}} + \gamma \dot{\widetilde{\mathbf{E}}} = \mathbf{0} \qquad (6.4.1)$$

See (Weidlinger Associates, 1991) for the derivation. Recognizing that the force exerted on a particle (or atom) of charge q_o in an electric field is

$$\mathbf{F} = q_o \widetilde{\mathbf{E}}$$

and that Newton's Second Law for the atom is

$$\mathbf{F} = m\ddot{\mathbf{u}}^{\alpha}$$

These two equations can be combined to create the equation

$$m\vec{\ddot{\mathbf{u}}}^{\alpha} = q_o \widetilde{\mathbf{E}}$$

or alternatively

$$\vec{\ddot{\mathbf{u}}}^{\alpha} = \widetilde{q}\widetilde{\mathbf{E}} \qquad (6.4.2)$$

where $\widetilde{q} = \dfrac{q_o}{m}$ and $\mathrm{m} = \dfrac{\left(0.48 \cdot mass(T_i) + 0.52 \cdot mass(Zr)\right)}{2}$ for the PZT at hand.

Consequently , equations (6.3.1), (6.4.1), and (6.4.2) constitute three equations and three unknowns which adequately describe the problem.

6.5 Variational Equations

Casting equations (6.3.1), (6.4.1), and (6.4.2) into the weak form – for a numerical solution by the finite element method – the problem is expressed mathematically as

$$\mathcal{G}_1 := \int_{S_t} \nabla \mathbf{w}^\beta : \boldsymbol{\sigma}(\mathbf{u}^\alpha, \mathbf{u}^\beta) dS_t - \int_{S_t} (\mathbf{w}^\beta \cdot \mathbf{b}) dS_t - \int_{\partial S_t} (\mathbf{w}^\beta \cdot \mathbf{t}) d\partial S_t - \int_{S_t} (\mathbf{w}^\beta \cdot \rho \ddot{\mathbf{u}}^\beta) dS_t = \mathbf{0}$$

With unknowns: $\{\mathbf{u}^\alpha, \mathbf{u}^\beta\}$

$$\mathcal{G}_2 := \int_{S_t} \mathbf{w}^\alpha \cdot (\rho \ddot{\mathbf{u}}^\alpha - \tilde{q}\tilde{\mathbf{E}}) dS_t = \mathbf{0}$$

With unknowns: $\{\mathbf{u}^\alpha, \tilde{\mathbf{E}}\}$

$$\mathcal{G}_3 := \int_{S_t} \mathbf{w}^E \cdot \left(\frac{1}{\mu} \nabla \times \nabla \times \tilde{\mathbf{E}} \right) dS_t + \int_{S_t} \mathbf{w}^E \cdot \left(\varepsilon \ddot{\tilde{\mathbf{E}}} + \gamma \dot{\tilde{\mathbf{E}}} \right) dS_t = \mathbf{0}$$

With unknown: $\{\tilde{\mathbf{E}}\}$

7 Conclusions & Future Work

7.1 Atomistic Elasticity Tensor

The elastic property tensor will be a $3 \times 3 \times 3 \times 3$ fourth order tensor which will have 81 *nontrivial* terms. All trivial/nontrivial terms and symmetries associated with the elastic tensor are determined solely by the crystal and are NOT prescribed a priori. The challenge for the PZT structure at hand will be to capture the behavior of the different types of atoms (which vary significantly) when formulating the elasticity tensor $\mathbf{C}$. Moreover, using the potential in Equation 5.2 (1) is meant merely as an illustrative example of the procedure since it neglects long range interactions common in piezoelectric materials.

7.1 Multiscale Formulation

Although the equations are all valid, issues concerning stability have not been addressed and will not be apparent until the stated weak form equations have been implemented and tested. Boundary conditions for $\mathbf{u}^\alpha$ and $\mathbf{u}^\beta$ also need to be addressed but can be modeled from earlier work in the field. An initial approach might be to use periodic boundary conditions for $\mathbf{u}^\alpha$ (used in most fine-scale molecular dynamics simulations), and boundary conditions typical of classic macro-scale solid mechanics for $\mathbf{u}^\beta$.

References

1. K. M. Rabe, Think locally, act globally, Nature Materials, 1 (2002) 147-148
2. Stillinger and Weber, PRB, v. 31, n. 8, 1985, p. 5262
3. J.R. Hughes, et. al. , The variational multiscale method – a paradigm for computational mechanics, Computer Methods in Applied Mechanics and Engineering, 166 (1998) 3-24
4. S.L. Creighton, R.A. Regueiro, K. Garikipati, P.A. Klein, E.B. Marin, D.J. Bammann, A variational multiscale method to incorporate strain gradients in a phenomenological plasticity model, Computer Methods in Applied Mechanics and Engineering, 193 (2004) 5453-5475
5. S.L. Creighton, Embedding models of finescale physics into the macromechanical continuum formulation of solid mechanics by variational multiscale techniques, Ph.D. thesis, University of Michigan, 2003.
6. D. Halliday and R. Resnick, Physics (Part II), John Wiley and Sons, 1978 ISBN 0-471-34529-6
7. Weidlinger Associates Inc., (1991) EMFlex Theory – Sections 1 and 2 http://www.wai.com/AppliedScience/Software/Emflex/Reports/emflextheory.pdf
8. M. A. Labo, S.M. Moraniec, D.J. Schoelles, Soldier Design Competition: Portable Power Generation System, Capstone Project (2005), Department of Civil and Mechanical Engineering, United States Military Academy.
* All pictures in this paper were either generated by the author or obtained by a public/free web search.